CRYSTAL HARDNESS AND AVERAGE DISTANCE BETWEEN STABLE–ENTANGLEMENTS IN MELT CRYSTALLIZED POLYETHYLENE

R.K. Bayer
Institut für Werkstofftechnik, Universität Kassel
Möncherbergstrasse 3. D-34125 Kassel, Germany.

F.J. Baltá Calleja
Instituto de Estructura de la Materia, CSIC
Serrano 119. E-28006 Madrid, Spain.

H.G. Kilian
Abteilung für Experimentelle Physik, Universität Ulm
Albert-Einstein-Allee 11. D-89069 Ulm, Germany.

Abstract Microhardness of a series of linear PE samples with a wide range of molecular weights has been determined. The influence of the mode of crystallization from the melt on the mechanical properties has been examined. It is shown that crystal hardness is correlated to the thickness of the amorphous layer for each series of samples. A new expression which describes the microhardness (H) of polyethylene as a function of the average distance between stable entanglements (knots) s is proposed. A value of $s = 360$Å, for the mean length between knots in the network is obtained. Analysis of data reveals that the H value can be expressed in terms of the following morphological parameters: 1) average number of chain folds in a lamellar crystal, 2) the nature of the interface between the crystalline and the amorphous layer and 3) the linear crystallinity.

Key words Microhardness, polyethylene, entanglements, amorphous layer.

Introduction

According to preceding studies [1-3], the hardness of the crystals of semicrystalline polymers with an average crystal thickness ℓ_c can be described as:

$$H_c = \frac{H_\infty}{(1 + \frac{b}{\ell_c})} \tag{1}$$

where H_∞ is the hardness value of infinite thick crystals and b is equal to $b = \frac{2\sigma}{\Delta H_f}$($\sigma$ is surface free energy and ΔH_f is the entalphy of crystal destruction). In a separate study [4] it was pointed out that the b parameter can be taken as a measure of the number of entanglements and other defects located at the crystal surface. It was further shown that b can vary depending on the nature of the surface which is directly controlled by molecular weight.

In the present investigation a series of samples of polyethylene were examined in which b varies between 140Å and 230Å. It will be shown that small values of b are correlated with correspondingly small values of the X–ray long period L. If one reduces the average molecular weight the number of entanglements at the crystal surface drastically diminishes leading to a decrease of the b–value. This effect is so pronounced that it overcompensates the influence of the concurrently diminishing crystal thickness upon H_c. The ratio $\frac{H_c}{H_\infty}$ decreases with increasing molecular weight in spite of the fact that ℓ_c increases.

The strong variation of the parameter b and its dominant influence on H_c, in comparison with the influence of crystal thickness, suggests a strong influence of the structure of the amorphous layer on H_c. One of us [5] has shown, that the thickness of the amorphous layer is an adequate measure for the molecular structure of the amorphous domains. Previous studies suggest that the amorphous layer consists of entanglements which are partly located on the crystal surface [6,7]. The

concentration of entanglements on the crystal surface strongly depends on crystallization conditions as we shall show below. Other entanglements form knots, which consist of a super–entanglements which are formed by chain–molecules which belong themselves to a network structure of entanglements. Knots can be, hence, seen as multifunctional chain couplings ($f \approx 250$). Molecular models show that these knots form the central part of the amorphous layer [5]. Forces are transmitted across the material by the knots through their multifunctional character. When a critical molecular weight $M_c' \approx 10^5$ is reached knots percolate, which means that their concentration comes to a saturation value. A critical amorphous thickness $\ell_a' = 90\text{Å}$ has been calculated for this critical molecular weight [5].

The aims of the present study are two-fold:
1) to propose a new analytical expression which includes not only the crystal thickness dependence on hardness but also which takes into account the amorphous thickness influence on this mechanical property;
2) to examine the origin of the correlation between hardness and the X–ray long period, the latter being modulated by the crystallization conditions.

Experimental

Sample preparation

Two series of commercial samples of polyethylene were prepared in the form of compression moulded plates. Commercial names and molecular weights are given in table 1. The first series of samples was prepared by slow cooling (4°C/min) of the molten materials to room temperature into plates a few mm thick (to be called S–series). The second series of samples was prepared by quenching thin layers of the

melt (0.5mm) into a cold water bath at a temperature of 4°C (Q–series).

Techniques

The microhardness was measured using a square diamond shape indenter. The hardness value was computed using the expression

$$H = \frac{K.P}{d^2} \tag{2}$$

where P is the applied load in N and d the projected diagonal length of the indentation in meters. K is a geometrical factor equal to 1.854. Loads of 0.05–0.1N were used. A loading cycle of 0.1min was applied. The small angle X–ray scattering patterns of the samples were investigated using a point collimation camera with a rotating anode Rigaku generator. The long period L was derived from the scattering maxima using Bragg's law after background subtraction. The volume degree of crystallinity α was calculated from density measurements.

Results

By assuming a two phase model we have calculated the crystal thickness $\ell_c = L\alpha$ and the thickness of the amorphous layer ℓ_a as $\ell_a = L - \ell_c$. The crystal hardness values H_c were derived from the measured H values using the relation $H \simeq H_c\alpha$ which applies for PE [3]. The b–parameter is obtained by inserting the values of H_c and ℓ_c in equation 1 and taking $H_\infty \simeq 170$ MPa from ref. 3. The experimentally measured H, L, and α values and the calculated $H_c, \frac{H_c}{H_\infty}, b, \ell_a$ and ℓ_c data for, both, quenched and slowly crystallized samples are collected in Tables 2 and 3.

Results show that for both series of materials, H, H_c and α decrease with molecular weight, and the ratio $\frac{H_c}{H_\infty}$ first decreases and then levels off with molecular weight, while b and ℓ_c gradually increase and finally

show a leveling off tendency. L increases with molecular weight over the range studied.

Fig. 1 shows the experimental values of ℓ_a for the quenched (Q) and slowly cooled samples (S) as a function of molecular weight. We have chosen the plot of ℓ_a against log M_η because the latter parameter characterizes the density of knots in the molten state [5,8] below M_c'. The quenched samples show slightly higher ℓ_a–values than the slowly crystallized samples. Since crystallization reduces the number of knots within the amorphous layer [5] the value of ℓ_a appears to be an adequate parameter to describe better the state of this amorphous layer than the value of log M_η. In what follows we shall discuss the variation of H_c, ℓ_c and b values as a function of ℓ_a (see Figs. 2 and 3). Fig. 2 shows the linear decrease of $\frac{H_c}{H_\infty}$ up to $\ell_a = 90$Å and the final constancy of the $H_c/H_\infty \sim 0.5$ for $\ell_a > 90$Å. Fig. 3 shows, on the other hand, the initial increase of b and ℓ_c with ℓ_a up to a given critical thickness $\ell_a' = 90$Å and, thereafter, the constancy of these values with further increasing ℓ_a. The straight lines drawn in Figs. 2 and 3 correspond to theoretical calculations of Baltá and Kilian [9].

Discussion

Influence of entanglement concentration at the crystal surface on microhardness

In a preceding investigation we have proposed a model to describe the development of the morphology of semicrystalline polymers upon cooling from the melt [5]. It was suggested that the molecular knots formed within the melt built up the central part of the amorphous layer. According to this model the defect surface of the crystals is described through a higher concentration of anchored entanglements on

this surface. During crystallization a parallelization of chain segments of the meshes of the entanglement network takes place. Simultaneously, the entanglements are pushed into the front of the emerging crystallite surfaces. The optimum crystalline geometry appears as that given by the average crystal thickness length which corresponds to the contour distance s_c between neighbouring entanglements within a chain in the melt. In this case the entanglements concentration on the crystals surface reaches a saturation value. Such an ideal structure is only obtained at a critical molecular weight ($M_\eta = M_c'$) for a slow rate of crystallization [5]. According to this model the longitudinal distance s between knots in the slowly crystallized polymer is equal to the average long period L:

$$L = s \simeq s_c + h_k = 358\text{Å} \tag{3}$$

where h_k is the thickness of the knot [5]. Thus, the case $L = s$ corresponds to a saturation of entanglements at the crystal surface. In general the L–value will depend on crystallization conditions. If $M_\eta < M_c'$ the concentration of entanglements at the crystal surface decreases and the parameter b concurrently diminishes with decreasing molecular weight [4]. On the other hand, if the molecular weight decreases, both, the crystal thickness and the thickness of the amorphous layer will also decrease. Furthermore, for $L = s$ the hardness of the crystals is equal to

$$H_c = \frac{1}{2} H_\infty \tag{4}$$

as we shall show below.

According to equation (1) H_c approaches H_∞, either when ℓ_c becomes large (for b=const) or when b becomes very small (for ℓ_c=const). The latter case means that H_c tends towards H_∞ the smaller is the

number of defects (entanglements) which are located at the crystal surface. The former case indicates that H_c tends to H_∞ the smaller is the ratio of the defect surface to the volume of the crystals. In summary, one can conclude that $H_c \rightarrow H_\infty$ when the absolute number of defects (entanglements) within the structure is minimum.

In the case of a saturation of defects at the surface ($L = s$) every chain that comes out from the crystal surface is involved in the formation of an entanglement. Let us assume the hypothetical case of a double number of entanglements per stem at the crystal surface. In this case, from entropy considerations, one may expect that every second entanglement per stem should tend to migrate towards the interior of each crystal. In other words, this situation corresponds to an unstable structure away from equilibrium which impedes the formation of the crystal. In this case, H_c would be equal to H_a. Hence for polyethylene such a supersaturation of defects would give a value $H_c \approx 0$.

We have seen that in the case $L = s$ the crystal defect surfaces are homogeneously covered by entanglements. Let us assume that in a "Gedanken–experiment" we would redistribute the entanglements in such a way that a given fraction of the entire crystal surface (one half $= 1 - \phi$) should have the double number of entanglements per stem ($H_c = 0$). Then, the other half (ϕ) of the crystal ought to remain completely free of defects ($H_c = H_\infty$). Consequently, for $L = s$ we could write:

$$H_c = \phi H_\infty = \frac{1}{2} H_\infty \tag{5}$$

In the case of $L < s$ ($M_\eta < M_c'$) the density of entanglements in the crystal surface decreases. Therefore, the fraction ϕ of crystals free of entanglements would increase according to

$$\phi = 1 - \frac{1}{2}\left(\frac{L}{s}\right) \tag{6}$$

By combination of equations 5 and 6 we obtain

$$\frac{H_c}{H_\infty} = 1 - \left(\frac{L}{2s}\right) \tag{7}$$

According to this expression, for large distances between knots ($s \gg L$), then $H_c = H_\infty$. On the other hand, for $L = s$; $\frac{H_c}{H_\infty} = \frac{1}{2}$. This value is obtained for the slow cooled samples when l_a reaches a critical value of 90Å($M_\eta = M_c'$) (see Fig. 2). This result supports the foregoing assumption that in case of a double saturation of entanglements at the crystal surface, $H_c = H_a = 0$. By using equation 7 we obtain from the H_c and L–data of the slow crystallized samples (Table 4) an average value of $s = 360$Å which agrees well with the value derived from the proposed model in ref. 5 (see equation 3).

From the H_c and L–data for the quenched samples (Table 5) a value of $s = 180$Å is obtained. From this result one may think that the density of knots in the case of the quenched samples should be twice as much as in the case of the slow crystallized samples. However, $s = 180$Å turns out to be half the value of $s = 360$Å, i.e. $s = 360/n_1$, (where $n_1 = 2$). This means that both s–values describe satisfactorily a constant knot density of the transferred network into the solid state. In this case n_1 represents the number of folds per stem which are present between adjacent knots in the crystallized polymer. In other words, in the case of quenched samples not only entanglements but also chain folds can be located on the crystal surface. The b–parameter derived for the quenched samples shows clearly smaller values than those for the slow crystallized samples. From previous studies [4] this result suggests that the density of entanglements at the crystal surface is smaller for the quenched samples. The occurrence of the folds explains why the average crystal thickness and the long period of the quenched samples are notably smaller than the values for the slow crystallized materials.

In general, the parameter n_1 can take values comprised between 1 and 2 depending on the crystallization conditions. Hence equation 7 can be written as

$$\frac{H_c}{H_\infty} = 1 - \left(\frac{Ln_1}{2s}\right) \tag{8}$$

thus relating the crystal hardness with the average distance between knots and taking into account, as well, the presence of chain folds.

By combination of equations 1 and 8 we obtain the expression:

$$\frac{\ell_c}{b} = \frac{2s}{L \cdot n_1} - 1 \tag{9}$$

which correlates the mechanical parameter b with the morphological parameters s and L.

Fig. 4 illustrates the plot of $\frac{\ell}{b}$ *vs* $\frac{1}{Ln_1}$ for calculated (solid line) and experimental data. According to eq. 9 the slope of the plot gives directly the distance between knots. The experimental data for $\frac{\ell}{b}$ show values below 1 for the quenched samples and values above 1 for the slowly cooled materials. The case $\frac{\ell_c}{b} = 1$ represents a structure in which the distance between knots according to equation 9, is equal to the long period.

Saturation of entanglements at the crystal surface

It has been indicated elsewhere [5] that $\ell'_{a_c} = 90$Å defines the percolation threshold of the knots in the case of well crystallized samples. Figs. 1–3 show that this also holds for the series of quenched samples (Q). Distinct change of the slope at a critical value $\ell'_{a_c} = 90$ is observed also for the Q–series. The constancy of the b–value above 90Å (Fig. 3) has been interpreted as a saturation level of entanglements on the crystal surfaces [3]. Thus, we can see that this concentration of entanglements coincides with the saturation level of knots within the

center of the amorphous phases ($\ell'_{a_c} = 90$Å). In addition, Fig. 3 seems to indicate that this saturation level depends on crystallization conditions. Indeed the Q–series exhibits lower b–values than the S–series which could suggest a lower entanglement concentration on the crystal surface.

According to eq. 7, the saturation level of entanglements in the crystal surface and knots within the amorphous phase should be correlated with a saturation level of the microhardness given by $s = L$. From eq. 7 this saturation level is described by $\frac{H_c}{H_\infty} = 0.5$. Indeed in Fig. 2 one observes that the variation of $\frac{H_c}{H_\infty}$ against ℓ_a characterizes satisfactorily this saturation value $\frac{H_c}{H_\infty} \approx 0.5$ of the microhardness for $\ell_a \geq \ell'_{a_c}$. For ℓ_a values smaller than 90Å, values of $\frac{H_c}{H_\infty}$ larger than 0.5 are observed. This result is connected with a decrease of the concentration of entanglements in the crystal surface as illustrated for the quantity b in Fig. 3. This situation is given, when $L < s$ (Fig. 4).

Reduced parameters

A closer inspection of Fig. 2 shows that for slowly crystallized samples the leveling off hardness value is given by $(\frac{H_c}{H_\infty})_{sat} = 0.53$ for $\ell_a \geq 90$Å while for the quenched samples, for $\ell_a \geq 90$Å one obtains $(\frac{H_c}{H_\infty})_{sat} = 0.49$. From eq. 8 one sees that the leveling–off of the microhardness is not accurately given by $s = L.n_1$ but by

$$s = k.L.n_1 \tag{10}$$

where $k = 1.06$ for the S–series and k=0.89 for the Q–series. Hence, it appears that $s = L$ does not represent accurately enough the criterion for the level of saturation of entanglements . It seems that

$$\ell_a = 90\text{Å} = \ell'_{a_c} \tag{11}$$

is a better criterion. By combination of eqs. 10 and 11 one obtains a saturation value for the crystalline thickness given by

$$\ell_{sat} = (L - \ell_a)_{sat} = \frac{s}{k.n_1} - 90\text{Å} \tag{12}$$

If $L \cdot n_1 = s$ would hold as criterion for the saturation level a reduced quantity ℓ_{redsat}

$$\ell_{redsat} = \frac{s}{n_1} - 90\text{Å} \tag{13}$$

would define the limiting value of crystal thickness. In the case of the Q–series ($n_1 = 2$) one expects a limiting value of $\ell_{redsat} = 90$Å. However, an experimental value of $\ell_{sat} = 120$Å is observed, which agrees with data from other authors on quenched PE samples [10] (see Fig. 3). If one applies eqs. 12 and 13 to the S–series one sees that $\ell_{sat} = 265$Å is lower than the expected value $\ell_{redsat} = 270$Å. Hence, the deviations of the microhardness from the expected values can be explained by a stronger crystal growth than it would correspond to $s = n_1/L$ in the case of the Q–series. A lower crystal thickness value in the case of the S–series is obtained. The different crystal thickness values can be taken into account by introducing a parameter β^{x}

$$\beta^{\mathrm{x}} = \frac{\ell_{redsat}}{\ell_{sat}} \tag{14}$$

According to this equation, for the Q–series we have $\beta^{\mathrm{x}} = 90\text{Å}/120\text{Å} = 0.75$ and for the S–series $\beta^{\mathrm{x}} = 270\text{Å}/265\text{Å} = 1.05$ (Fig. 2). It is now convenient to define a reduced long period as

$$L_{red} = \beta^{\mathrm{x}}\ell + \ell_a \tag{15}$$

If we now introduce in eq. 8 the value of L_{red} we obtain a reduced value for the hardness:

$$\left(\frac{H_c}{H_\infty}\right)_{red} = 1 - \frac{L_{red}.n_1}{2s} \tag{16}$$

Fig. 5 shows the calculated reduced H_c–values for both series of samples as a function of ℓ_a for $\ell_a \leq \ell'_{a_c}$. The substitution of L by L_{red} leads to a master curve of the microhardness described by eq. 16. While the experimental data of $\frac{H_c}{H_\infty}$ for both Q and S–series differ from each other (Fig. 2) the calculated reduced H–values show the same results for both series.

The criterion for the saturation level of the hardness $\ell_a = \ell'_{a_c} = 90\text{Å}$ coincides now with the saturation level of entanglements in the crystal surface: $s = 360\text{Å} = L_{red}$. From eq. 16 one obtains: $\left(\frac{H_c}{H_\infty}\right)_{red} = 0.5$, a criterion which now strictly applies for $\ell'_{ac} = 90\text{Å}$ (Fig. 4).

We have seen that the β^x parameter defines a master curve. According to eq. 15, the parameter β^x measures the relative capability of the growing crystal to reach a limiting value ℓ_{redsat} against the constraining effect of the network of entanglements and knots. In case of the Q–series the crystallization capability defined by ℓ_{sat} exceeds the $(\ell_{sat})_{red}$–value and β^x shows up a value of 0.75. This is due to the presence of a low density of entanglements on the crystal surface. On the contrary, in the case of the S–series showing substantially larger ℓ_c–values (Fig. 5), $\beta^x = 1.05$. In this case, the ℓ_{redsat} value is not quite reached. Here the resistance to the growing of the crystal due to the presence of entanglements is larger than in the former case (density of entanglements at the crystal surface is higher). The above results indicate that β^x parameter offers information about the structure of the interface.

Reduced hardness values below l'_a

We have seen that eq 12 describes the saturation level of entanglements in the crystal–surfaces which depends on cooling conditions (n_1). For $k = 1$ it results

$$L_{red_{sat}} = \frac{s}{n_1} \tag{17}$$

The saturation level of entanglements at the crystal surface is characterized by $\ell_a = \ell'_{a_c} = 90\text{Å}$ which is equivalent to the percolation condition of knots ($M_\eta = M'_c$). For molecular weights lower than M'_c, L_{red} decreases below the value of eq. 17. This value is equivalent to the increase of $\left(\frac{H_c}{H_\infty}\right)_{red}$ below M'_c to values larger than 0.5 (Fig. 5). In analogy with eq. 17 this may be described by an introduction of additional chain folds defined by a parameter n_2:

$$L_{red} = \frac{s}{n_1 n_2} \tag{18}$$

Using eq. 16 we obtain

$$(H_c/H_\infty)_{red} = 1 - \frac{1}{2n_2} \tag{19}$$

which indicates, that n_2 is the only parameter which defines the reduced hardness. Fig. 6 shows the plot of n_2, calculated from eq. 19, for $\ell_a < 90\text{Å}$, as a function ℓ_a.

By inspection of eq. 19 one sees that for $n_2 = 1$ one obtains a value which corresponds to the saturation limit of entanglements in the crystal surface. However, for $\ell_a \leq 90\text{Å}$ one obtains values of $n_2 > 1$, which means that as ℓ_a decreases, the number of chain folds increases (Fig. 5). This is provided by the decrease of the knot–density below $M'_c = 10^{5.2}$ (ref. [11]). Hence an increase of n_2 for $M_\eta < M'_c$ expresses the decrease of the knot density. Thus, n_2 is correlated to the knot density within the center of the amorphous phase.

By combination of eqs. 15 and 18 and $\ell_c = \alpha L$, and using the expression $\ell_a = (1-\alpha)L$ one obtains

$$L = \frac{s}{n_1 n_2} \quad \frac{1}{\alpha(\beta^x - 1) + 1} \tag{20}$$

which describes the dependency of the long period from the various physical parameters. If we insert eq 20 into 8 we obtain a final expression for the hardness.

$$\frac{H_c}{H_\infty} = 1 - \frac{1}{2n_2} \cdot \frac{1}{\alpha(\beta^x - 1) + 1} \tag{21}$$

which is a function of two principal parameters: n_2 which depends on molecular weight and gives a measure of the knot density in the amorphous phase and β^x which describes the quality of the amorphous interface.

Conclusions

In conclusion, a relationship between the crystal hardness (H_c) and the thickness of the amorphous layer (ℓ_a) has been obtained for melt crystallized linear PE samples. The H_c–values are shown to depend strongly on the crystallization conditions. It is shown that the density of knots and the crystallization mode control the b–mechanical parameter. The latter is proportional to the number of entanglements at the surface layer. It is further found that b increases with ℓ_a and that for $\ell_a = 90$Å, the saturation level of entanglements on the crystal surface coincides with the percolation level of knots in the amorphous layer. Finally, results indicate that the density of knots in the amorphous layer influence the morphology and, hence, the mechanical properties

through H_c. This dependence is illustrated in terms of an equation which correlates H_c with the X–ray long period.

Acknowledgements

Thanks are due to DGICYT (Grant PB94-0049), Spain, and to NEDO's International Joint Research Program, Japan, for the generous support of this investigation. We thank C. Santa Cruz for the determination of the experimental microhardness values.

References

[1] Baltá Calleja FJ, Kilian HG (1988) Colloid & Polym. Sci. 266: 29

[2] Deslandes Y, Alva Rosa E, Brise F, Mecreghim J (1991) J. Mater. Sci. 26: 2769

[3] Baltá Calleja FJ (1994) Trends in Polym. Sci. 2(12): 419

[4] Baltá Calleja FJ, Santa Cruz C, Bayer RK, Kilian HG (1990) Colloid & Polym. Sci. 268: 440

[5] Bayer RK (1994) Colloid & Polym. Sci. 272: 910

[6] Holl B, Heise B, Kilian HG (1983) Colloid & Polym. Sci. 261: 978

[7] Mandelkern L, Alamo RG, Kennedy MA (1990) Macromolecules 23: 4721

[8] Bayer RK, Baltá Calleja FJ, López Cabarcos E, Zachmann HG, Paulsen A, Bruning F, Meins W (1989) J. Mater. Sci. 24: 2643

[9] Kilian HG, Baltá Calleja FJ (unpublished results)

[10] Rault J, Robelin-Souffeché E (1989) J.Polym. Sci.; Polym. Phys. 27: 1349

[11] Bayer RK, Liebentraut F, Meyer T (1992) Colloid & Polym Sci. 270: 331

LEGEND TO FIGURES

Fig. 1 Average thickness of the amorphous layer (ℓ_a) as function of *log* M_η for quenched (Q) and slowly cooled (S) PE samples.

Fig. 2 The ratio H_c/H_∞ for the Q and S–series as a function of ℓ_a. The continuous straight lines correspond to calculated values [9].

Fig. 3 Average crystal thickness ℓ_c and b–parameter as function of ℓ_a for the quenched (Q) and the slowly cooled (S) PE samples.

Fig. 4 Plot of ℓ_c/b *vs* $1/n_1 L$ for calculated (solid line) and experimental data.

Fig. 5 Master curve for the reduced ratio $(H_c/H_\infty)_{red}$ of the Q and S series.

Fig. 6 Plot of the n_2 parameter as function of ℓ_a.

Table 1 Polyethylene materials investigated

Commercial name	M_η
Vestolen A 6016	56.000
Vestolen A 6013	88.000
Rigidex 6006-60	115.000
Lupolen 6021 D	161.000
Lupolen 5661 B	173.000
Lupolen 5261 Z	248.000
Hostalen GR6255	307.000
Hostalen GR400	2×10^6

Table 2 Experimental values of microhardness H, crystal hardness H_c, ratio H_c/H_∞, mechanical parameter b, long period L, thickness of the amorphous layer ℓ_a, crystal thickness ℓ_c and crystallinity α for the **quenched PE** samples as a function of increasing M_η.

$logM_\eta$	$H(MPa)$	$H_c(MPa)$	$\frac{H_c}{H_\infty}$	b(Å)	L(Å)	ℓ_a(Å)	ℓ_c(Å)	α
4.75	50.7	79.8	0.47	126	185	74	111	0.60
4.94	48.3	79.1	0.47	131	198	84	114	0.58
5.06	48.1	79.3	0.47	137	208	90	118	0.57
5.21	45.2	75.6	0.44	147	208	90	111	0.57
5.24	45.2	75.8	0.45	148	212	93	114	0.56
5.39	43.3	76.5	0.45	148.5	229	108	118	0.53
5.49	42.7	76.5	0.45	151	236	112	118	0.53
6.3	32.8	76.1	0.45	146	279	161	119	0.42

Table 3 Same values as in Table 2 for the **slowly cooled PE** samples

$log M_\eta$	$H(MPa)$	$H_c(MPa)$	$\frac{H_c}{H_\infty}$	b(Å)	L(Å)	ℓ_a(Å)	ℓ_c(Å)	α
4.75	76	97.3	0.57	157	281	70	211	0.75
4.94	73	95.7	0.56	179	311	80	231	0.74
5.06	73	94.7	0.55	193	323	82	241	0.75
5.21	69	89.8	0.53	220	334	87	247	0.74
5.24	69	89.8	0.53	223	340	89	251	0.74
5.39	68	92.3	0.54	224	375	108	267	0.71
5.49	67	91.7	0.54	225	376	114	262	0.70

Table 4 Average distance between knots along the chains, s, for the slowly cooled PE samples (S–Series). $\bar{s}$ denotes the mean value of the obtained data.

M_η	s/Å	
56.000	327	
88.000	353	$\bar{s} = 360$ Å
115.000	359	
161.000	362	
173.000	361	

Table 5 s–values derived for the quenched PE samples Q–Series

M_η	s/Å	n_1	
56.000	175	2.06	
88.000	187	1.92	
115.000	196	1.83	$\bar{s} = 180$Å
161.000	186	1.94	
173.000	193	1.86	

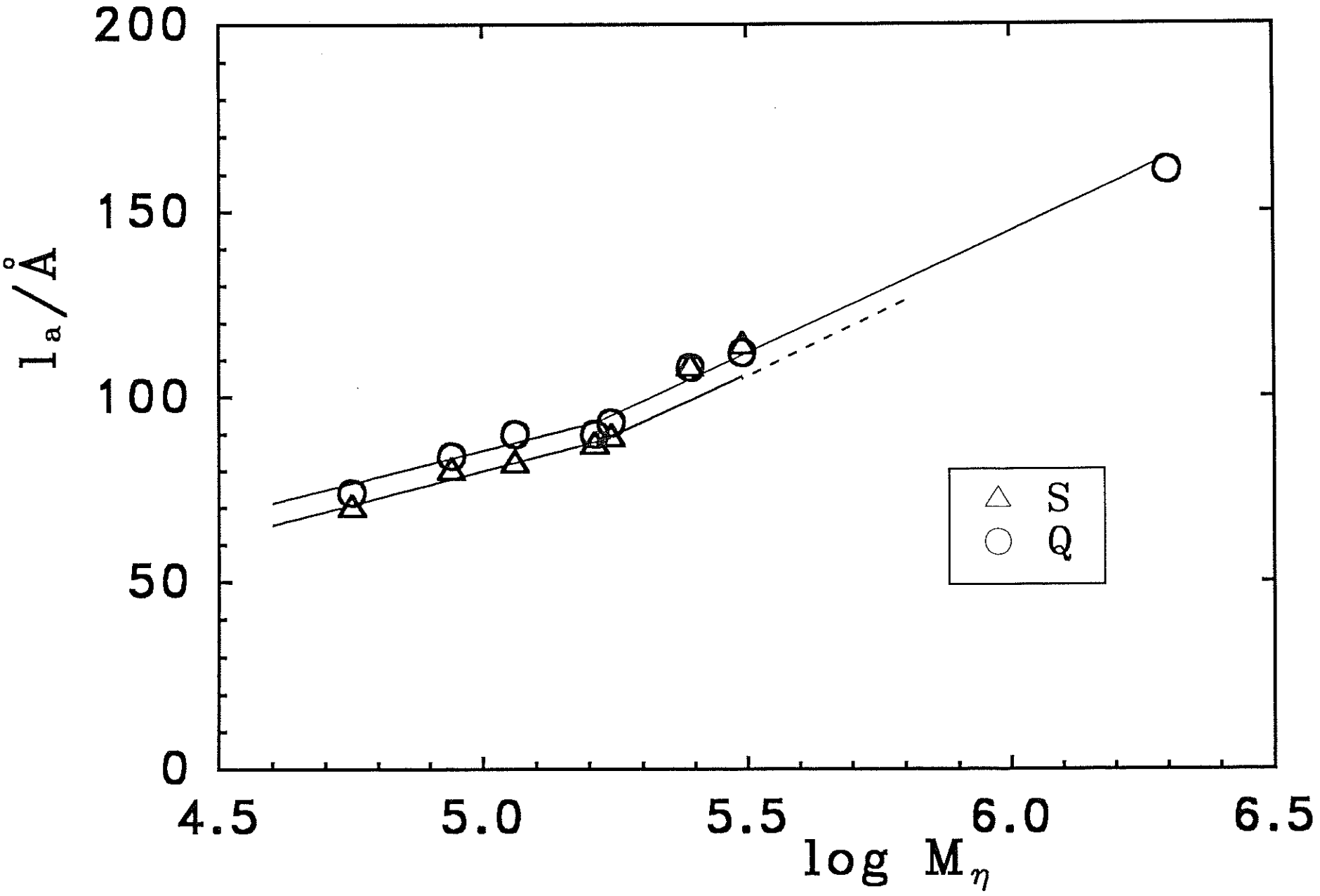

Fig 1

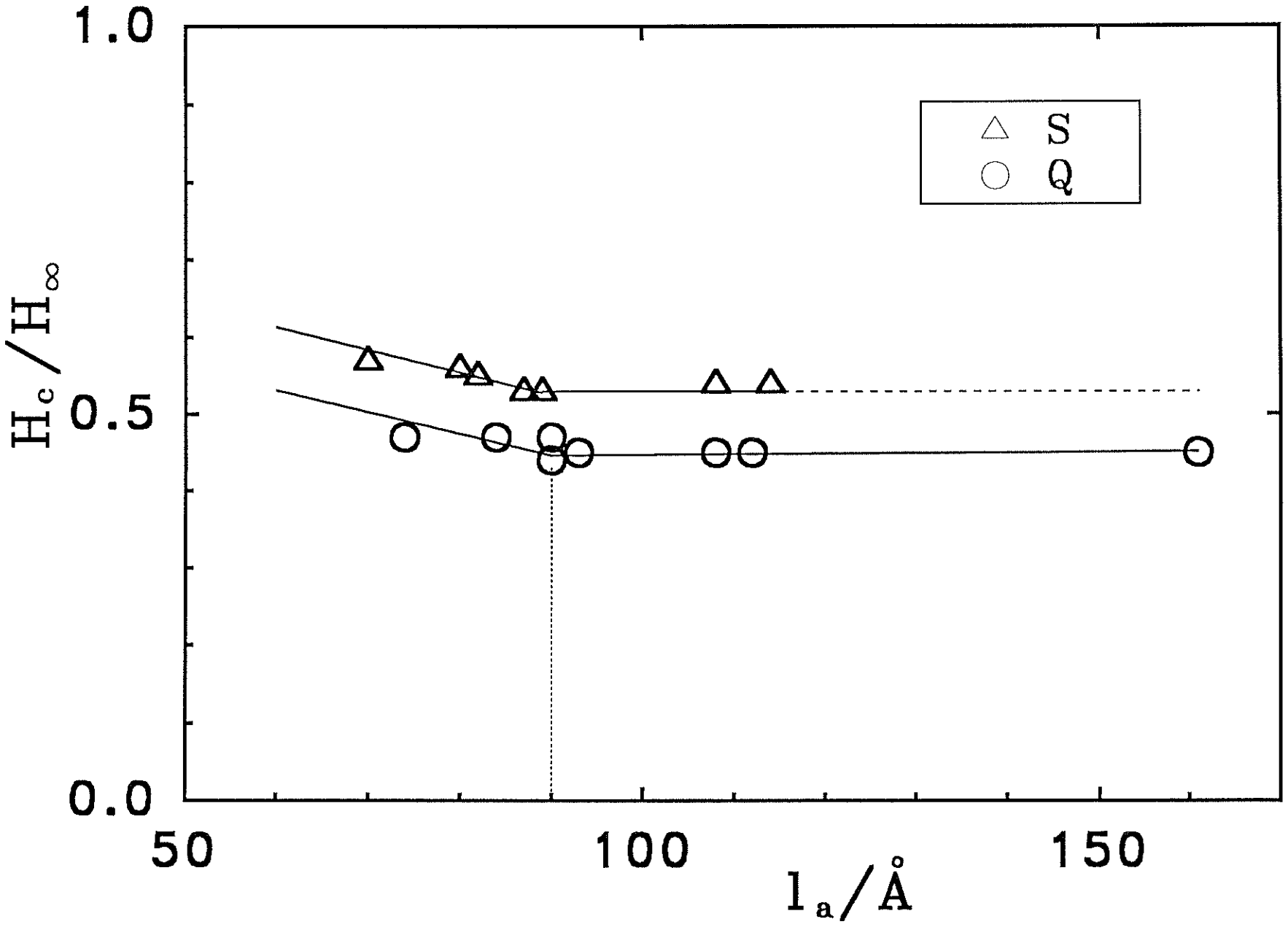

Fig 2

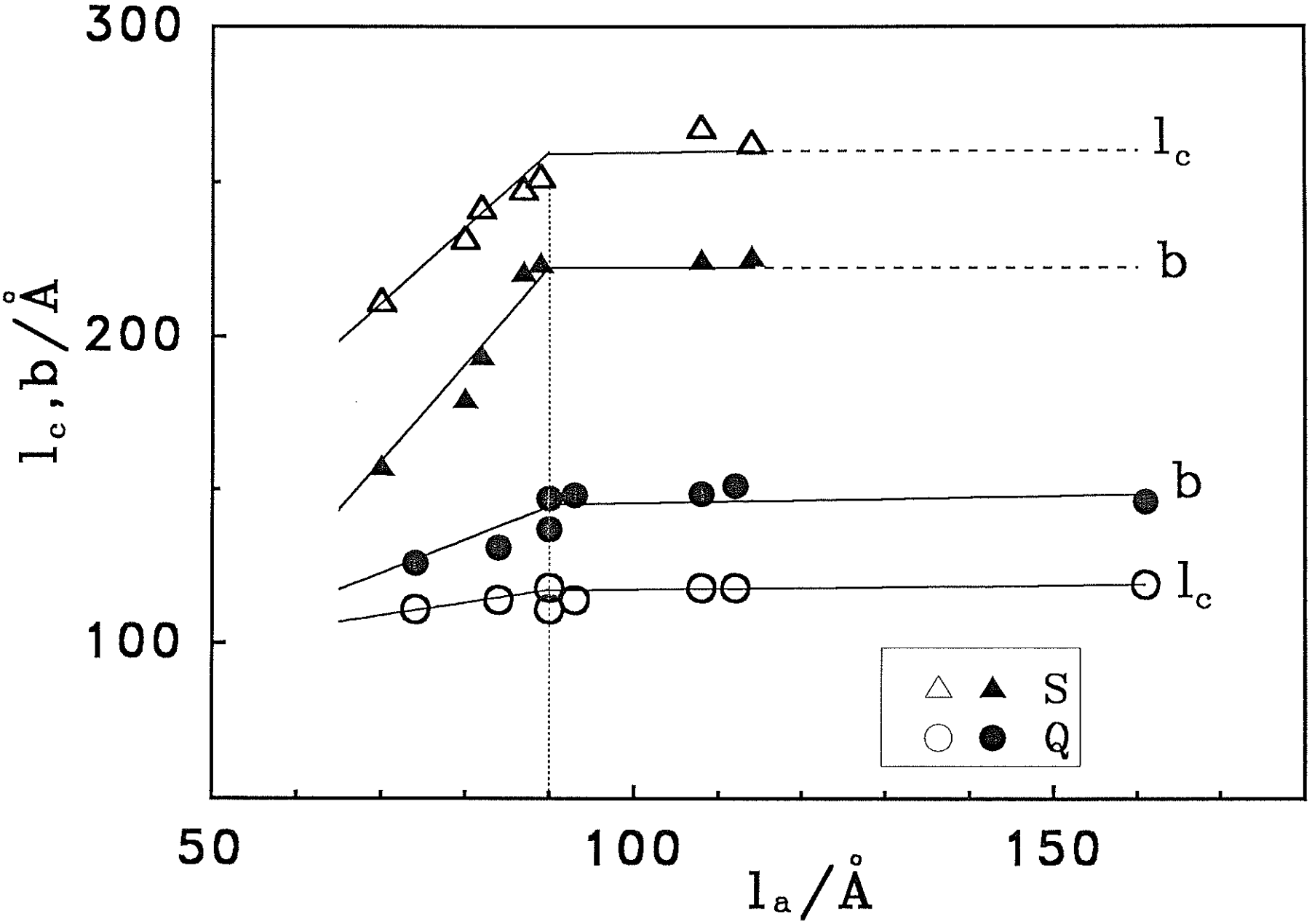

Fig. 3

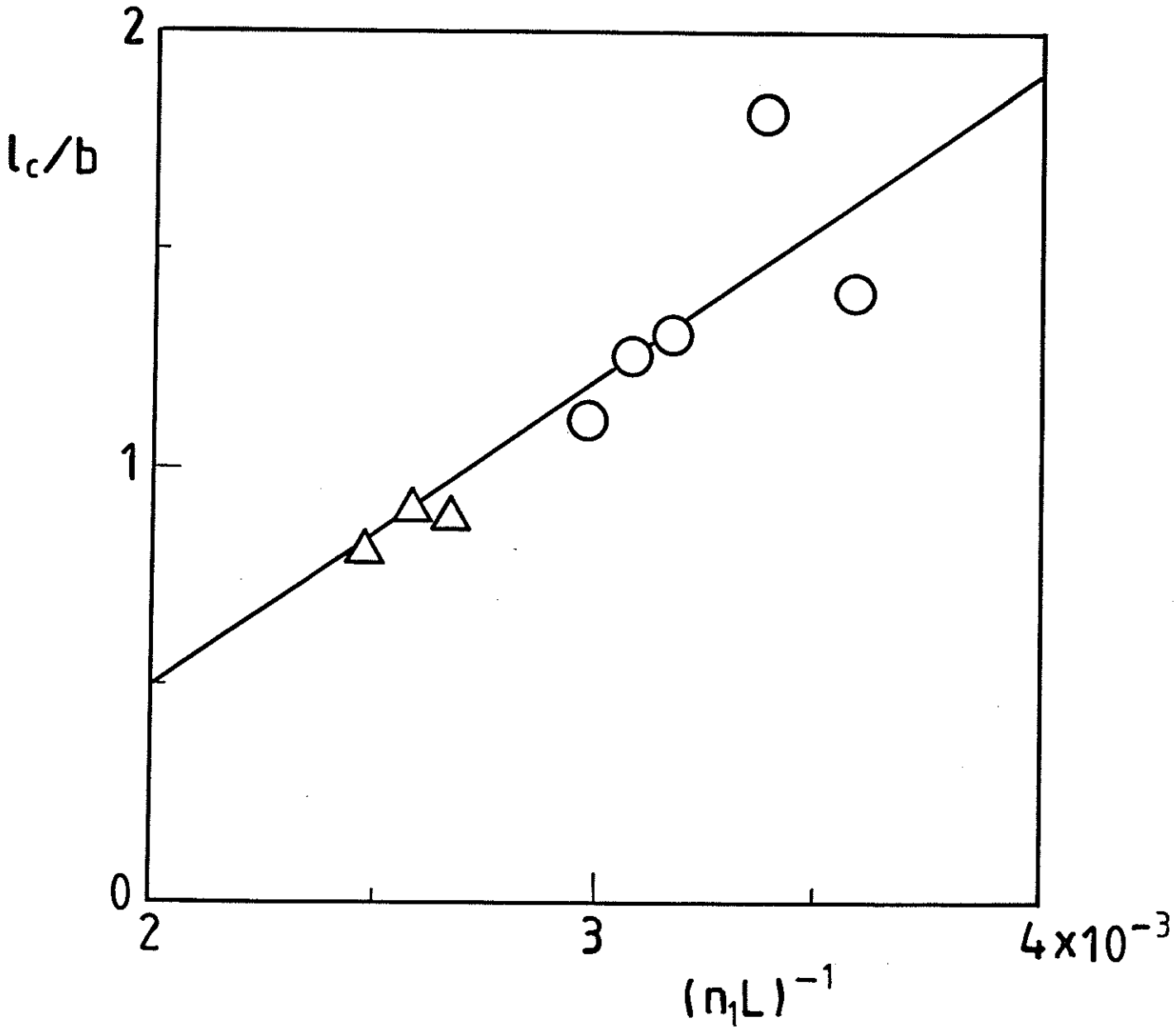
2
1
0
l_c/b
2
3
4×10^{-3}
$(n_1L)^{-1}$

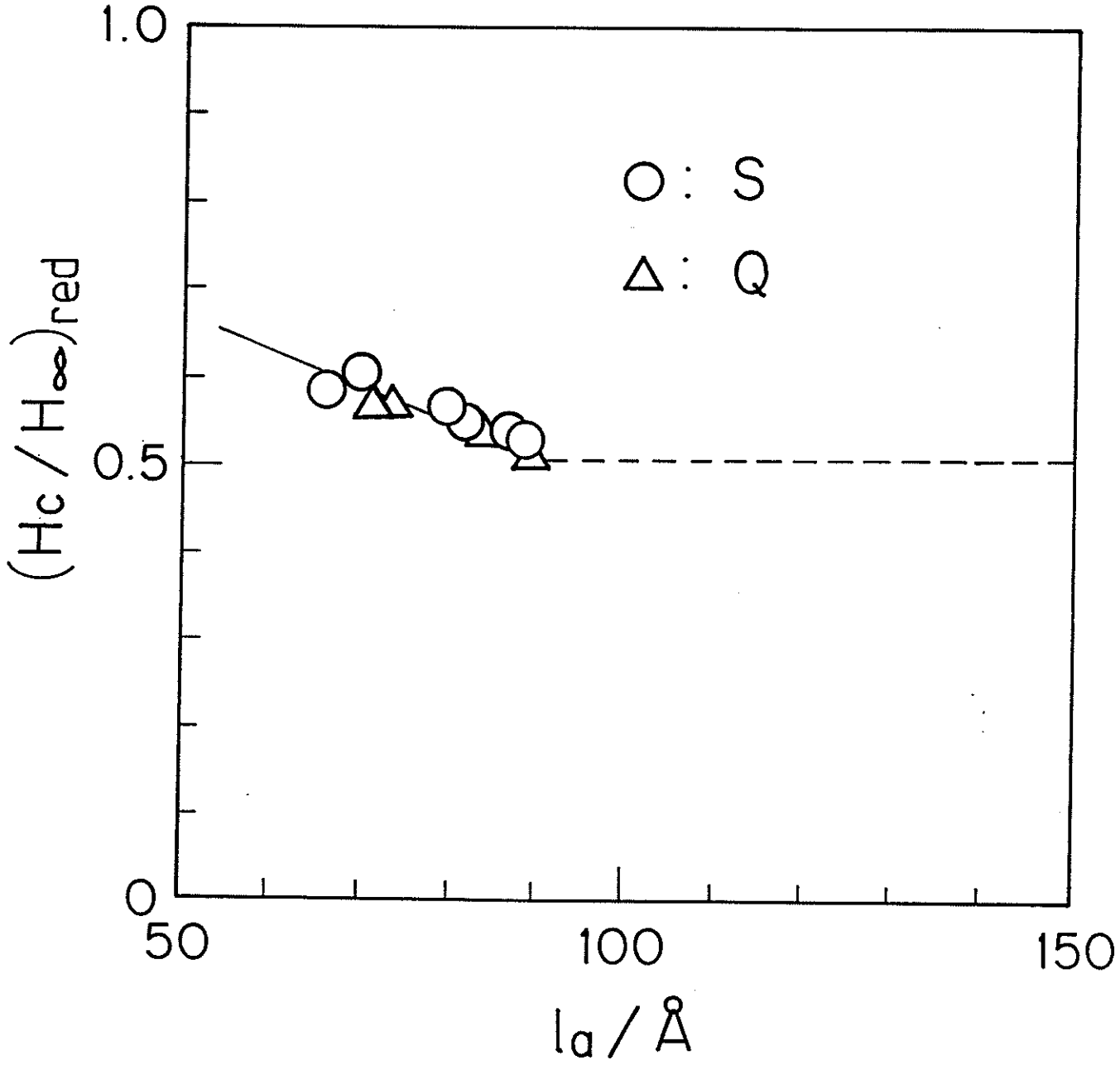

Fig 5

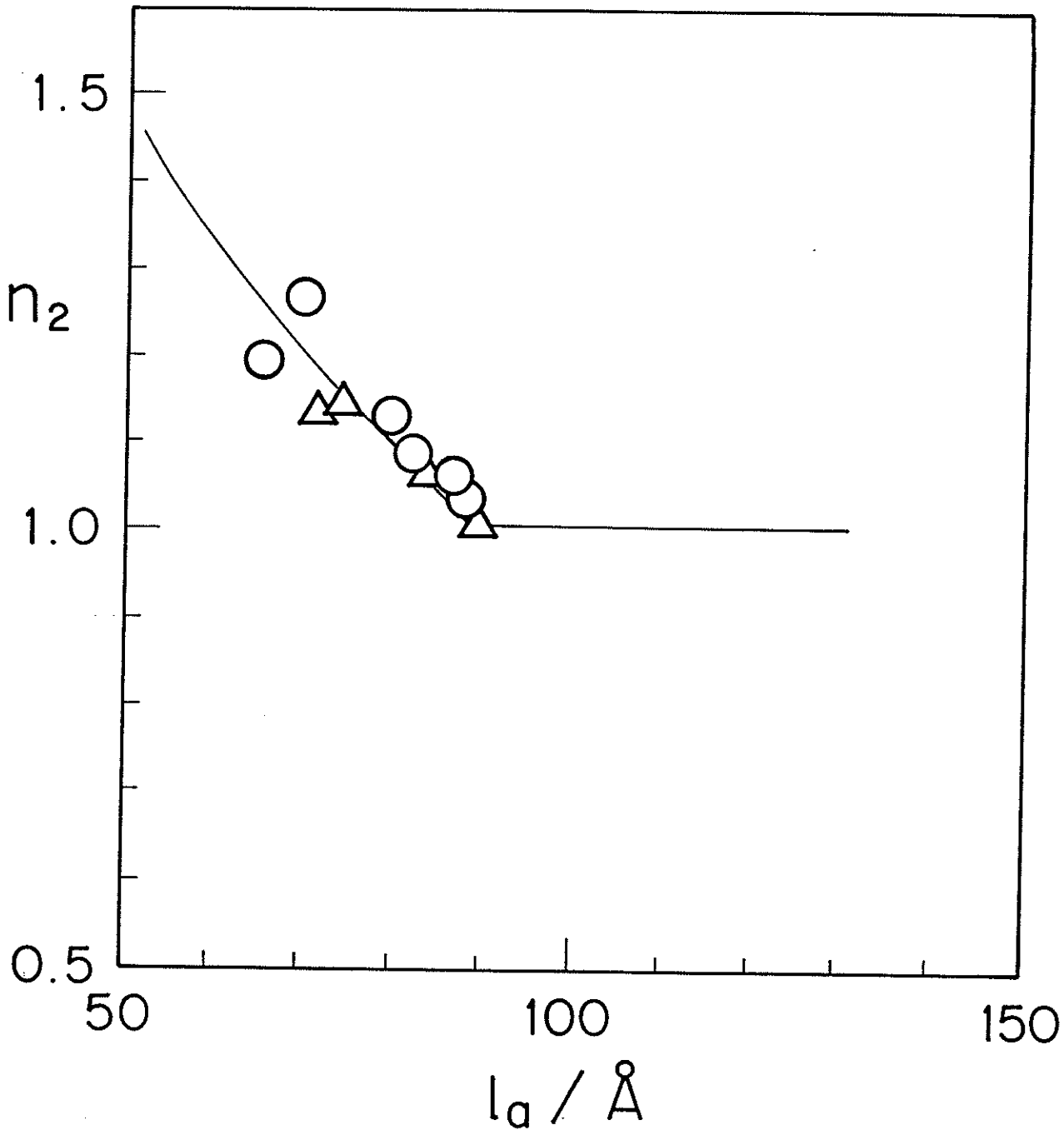

Fig 6